18. P. Mészáros, *Rep. Prog. Phys.* **69**, 2259–2321 (2006).
19. G. Ghisellini, M. Nardini, G. Ghirlanda, A. Celotti, *Mon. Not. R. Astron. Soc.* **393**, 253–271 (2009).
20. A. Panaitescu, W. T. Vestrand, *Mon. Not. R. Astron. Soc.* **414**, 3537–3546 (2011).
21. R. Sari, T. Piran, J. P. Halpern, *Astrophys. J.* **519**, L17–L20 (1999).
22. H. van Eerten, W. Zhang, A. MacFadyen, *Astrophys. J.* **722**, 235–247 (2010).
23. H. J. van Eerten, A. I. MacFadyen, *Astrophys. J.* **751**, 155 (2012).
24. L. Nava, L. Sironi, G. Ghisellini, A. Celotti, G. Ghirlanda, *Mon. Not. R. Astron. Soc.* **433**, 2107–2121 (2013).
25. H. van Eerten, A. van der Horst, A. MacFadyen, *Astrophys. J.* **749**, 44 (2012).
26. R. Liu, X. Wang, X. Wu, *Astrophys. J. Lett.* **773**, L20 (2013).
27. P.-H. T. Tam, Q.-W. Tang, S.-J. Hou, R.-Y. Liu, X.-Y. Wang, *Astrophys. J.* **771**, L13 (2013).
28. L. Amati *et al.*, *Astron. Astrophys.* **390**, 81–89 (2002).
29. D. Yonetoku *et al.*, *Astrophys. J.* **609**, 935–951 (2004).
30. G. Ghirlanda, G. Ghisellini, D. Lazzati, *Astrophys. J.* **616**, 331–338 (2004).
31. T. Laskar *et al.*, *Astrophys. J.* **776**, 119 (2013).

Acknowledgments: This work has been supported by ASI grant I/004/11/0 and by Progetto di Ricerca di Interesse Nazionale (PRIN)–Ministero dell'Istruzione, dell'Università e della Ricerca (MIUR) grant 2009ERC3HT. Development of the BOXFIT code (*25*) was supported in part by NASA through grant NNX10AF62G issued through the Astrophysics Theory Program and by the NSF through grant AST-1009863. This research was partially supported by the Ministry of Education, Culture, Sports, Science and Technology of Japan (MEXT), grants-in-aid 14GS0211, 19047001, 19047003, and 24740186. The Liverpool Telescope is operated by Liverpool John Moores University at the Observatorio del Roque de los Muchachos of the Instituto de Astrofísica de Canarias. The Faulkes Telescopes, now owned by Las Cumbres Observatory, are operated with support from the Dill Faulkes Educational Trust. Swift support at the University of Leicester and the Mullard Space Science Laboratory is funded by the UK Space Agency. C.G.M. acknowledges financial support from the Royal Society, the Wolfson Foundation, and the Science and Technology Facilities Council. A.G. acknowledges funding from the Slovenian Research Agency and from the Centre of Excellence for Space Sciences and Technologies SPACE-SI, an operation partly financed by the European Union, European Regional Development Fund, and Republic of Slovenia. DARK is funded by the Danish National Research Foundation.

Supplementary Materials
www.sciencemag.org/content/343/6166/48/suppl/DC1
Materials and Methods
Supplementary Text
Figs. S1 to S7
Tables S1 to S10
References (*32*–*62*)

21 June 2013; accepted 16 October 2013
Published online 21 November 2013;
10.1126/science.1242279

The First Pulse of the Extremely Bright GRB 130427A: A Test Lab for Synchrotron Shocks

R. Preece,[1*] J. Michael Burgess,[2*] A. von Kienlin,[3*] P. N. Bhat,[2] M. S. Briggs,[2] D. Byrne,[4] V. Chaplin,[2] W. Cleveland,[5] A. C. Collazzi,[6,7] V. Connaughton,[2] A. Diekmann,[8] G. Fitzpatrick,[4] S. Foley,[4,3] M. Gibby,[8] M. Giles,[8] A. Goldstein,[6,7] J. Greiner,[3] D. Gruber,[3] P. Jenke,[2] R. M. Kippen,[9] C. Kouveliotou,[6] S. McBreen,[4,3] C. Meegan,[2] W. S. Paciesas,[5] V. Pelassa,[2] D. Tierney,[4] A. J. van der Horst,[10] C. Wilson-Hodge,[6] S. Xiong,[2] G. Younes,[5,6] H.-F. Yu,[3] M. Ackermann,[11] M. Ajello,[12] M. Axelsson,[13,14,15] L. Baldini,[16] G. Barbiellini,[17,18] M. G. Baring,[19] D. Bastieri,[20,21] R. Bellazzini,[22] E. Bissaldi,[23] E. Bonamente,[24,25] J. Bregeon,[22] M. Brigida,[26,27] P. Bruel,[28] R. Buehler,[11] S. Buson,[20,21] G. A. Caliandro,[29] R. A. Cameron,[30] P. A. Caraveo,[31] C. Cecchi,[24,25] E. Charles,[30] A. Chekhtman,[32] J. Chiang,[30] G. Chiaro,[21] S. Ciprini,[33,34] R. Claus,[30] J. Cohen-Tanugi,[35] L. R. Cominsky,[36] J. Conrad,[37,14,38,39] F. D'Ammando,[40] A. de Angelis,[41] F. de Palma,[26,27] C. D. Dermer,[42*] R. Desiante,[17] S. W. Digel,[30] L. Di Venere,[30] P. S. Drell,[30] A. Drlica-Wagner,[30] C. Favuzzi,[26,27] A. Franckowiak,[30] Y. Fukazawa,[43] P. Fusco,[26,27] F. Gargano,[27] N. Gehrels,[44] S. Germani,[24,25] N. Giglietto,[26,27] F. Giordano,[26,27] M. Giroletti,[40] G. Godfrey,[30] J. Granot,[45] I. A. Grenier,[46] S. Guiriec,[44,7] D. Hadasch,[29] Y. Hanabata,[43] A. K. Harding,[44] M. Hayashida,[30,47] S. Iyyani,[14,15,37] T. Jogler,[30] G. Jóannesson,[48] T. Kawano,[43] J. Knödlseder,[49,50] D. Kocevski,[30] M. Kuss,[22] J. Lande,[30] J. Larsson,[15,14] S. Larsson,[37,14,13] L. Latronico,[51] F. Longo,[17,18] F. Loparco,[26,27] M. N. Lovellette,[42] P. Lubrano,[24,25] M. Mayer,[11] M. N. Mazziotta,[27] P. F. Michelson,[30] T. Mizuno,[52] M. E. Monzani,[30] E. Moretti,[15,14] A. Morselli,[53] S. Murgia,[30] R. Nemmen,[44] E. Nuss,[35] T. Nymark,[15,14] M. Ohno,[54] T. Ohsugi,[52] A. Okumura,[30,55] N. Omodei,[30*] M. Orienti,[40] D. Paneque,[56,30] J. S. Perkins,[44,57,58] M. Pesce-Rollins,[22] F. Piron,[35] G. Pivato,[21] T. A. Porter,[30] J. L. Racusin,[44] S. Rainò,[26,27] R. Rando,[20,21] M. Razzano,[22,59] S. Razzaque,[60] A. Reimer,[23,30] O. Reimer,[23,30] S. Ritz,[59] M. Roth,[61] F. Ryde,[15] A. Sartori,[31] J. D. Scargle,[62] A. Schulz,[11] C. Sgrò,[22] E. J. Siskind,[63] G. Spandre,[22] P. Spinelli,[26,27] D. J. Suson,[64] H. Tajima,[30,55] H. Takahashi,[43] J. G. Thayer,[30] J. B. Thayer,[30] L. Tibaldo,[30] M. Tinivella,[22] D. F. Torres,[29,65] G. Tosti,[24,25] E. Troja,[44,66] T. L. Usher,[30] J. Vandenbroucke,[30] V. Vasileiou,[35] G. Vianello,[30,67] V. Vitale,[53,68] M. Werner,[23] B. L. Winer,[69] K. S. Wood,[42] S. Zhu[66]

Gamma-ray burst (GRB) 130427A is one of the most energetic GRBs ever observed. The initial pulse up to 2.5 seconds is possibly the brightest well-isolated pulse observed to date. A fine time resolution spectral analysis shows power-law decays of the peak energy from the onset of the pulse, consistent with models of internal synchrotron shock pulses. However, a strongly correlated power-law behavior is observed between the luminosity and the spectral peak energy that is inconsistent with curvature effects arising in the relativistic outflow. It is difficult for any of the existing models to account for all of the observed spectral and temporal behaviors simultaneously.

In the context of Gamma-ray burst (GRB) 130427A, which triggered the Gamma-Ray Burst Monitor (GBM) (*1*) on the Fermi Gamma-Ray Space Telescope on 27 April 2013 at T_0 = 07:47:06.42 UTC (*2*–*4*) is an extreme case. The peak flux on the 64-ms time scale is 1300 ± 100 photons s^{-1} cm^{-2} in the 10 to 1000 keV range and the fluence, integrated over the same energy range and a total duration of ~350 s, is (2.4 ± 0.1) × 10^{-3} erg cm^{-2}. The longest continuously running GRB detector, Konus on the Wind spacecraft, has been observing the entire sky for nearly 18 years, and only one burst had a larger peak flux, by ~30% (GRB 110918A) (*5*). GRB 130427A is the most fluent burst in the era starting with the 1991 launch of the Burst and Transient Source Experiment (BATSE) on the Compton Gamma-Ray Observatory. Finally, the energy of the spectral peak in the first time bin (T_0 – 0.1 to 0.0 s), 5400 ± 1500 keV, is the second highest ever recorded (*6*).

The initial pulse (Fig. 1), lasting up to 2.5 s after the trigger, stands on its own as being so bright (170 ± 10 photons s^{-1} cm^{-2} peak flux for 10 to 1000 keV in the 64-ms time bin at T_0 + 0.51 s) as to be ranked among the 10 brightest GBM or BATSE bursts (*7*–*9*). The brightness allows us to track the spectral evolution of the rising portion of a well-separated pulse with unprecedented detail (*10*). Evident in the GBM low-energy light curve [Fig. 1; as well as the 15 to 350 keV light curve presented in (*11*)] are fluctuations starting at around 1 s that are not present at higher energies. If these represent additional low-energy pulses, their presence clearly does not dominate the analyses presented below.

Past studies of time-resolved spectra of simple pulses in GRBs indicate that there are broadly two classes of spectral evolution. These are called "hard-to-soft" and "tracking" pulses (*12*, *13*), depending on whether the energy of the peak in the νF_ν spectrum (generically called E_{peak} herein) monotonically decays independently of the flux evolution or else generally follows the rise and fall of the flux. Typically, there are at most one or two spectra available for fitting during the rising portion of the flux history. What makes this event unique is that there are roughly six time bins with excellent counts statistics before the peak in the 10 to 1000 keV flux.

As seen in Fig. 1, there is a clear trend in the individual detector's light curves: the >20 MeV

Fermi Large Area Telescope (LAT) low-energy (LLE) (*14*, *15*) light curve peaks before the GBM trigger time (T_0), whereas the GBM bismuth germanate (BGO) detector #1 (300 keV to 45 MeV) and sodium iodide (NaI) detector #6 (8 to 300 keV) peak at successively later times. To quantify this, we performed an energy-dependent pulse lag analysis using a Discrete Cross Correlation Function (DCCF) and obtained the time lags τ (*16*) between the highest energy LAT LLE light curve and light curves at several selected energy ranges in the GBM NaI and BGO detectors (Fig. 1, inset). We find good agreement between the expected lag behavior and the pulse width model $W(E) \propto E^{\alpha}$ (*17*), obtaining a fitted value for $\alpha = -0.27 \pm 0.03$ (*18*). This model was previously fit to 400 pulses from 41 BATSE GRBs (*17*); an average value of $\alpha = -0.41$ was found. Synchrotron shock model simulations made by Daigne and Mochkovitch (*19*) found $\alpha \sim -0.4$ for pulses of 2- to 10-s duration, but $\alpha > \sim -0.2$ for pulses of 0.1 to 1 s. Three LAT photons with energies greater than 100 MeV are clustered in coincidence with the LLE peak, and so may arise by the same mechanism.

Although most GRB spectra are well fit by the smoothly joined broken power-law function of Band *et al*. (*20*), in some cases the simultaneous fit of a Band function together with an additional blackbody component is significantly better statistically (*6*, *21*, *22*). Burgess *et al*. (*23*, *24*) also noted the requirement of an additional blackbody component but replaced the phenomenological Band function with a physically motivated synchrotron function. We present two separate time-resolved spectral analyses for the first 2.5 s of GRB 130427A, with comparable goodness of fit: the Burgess *et al*. synchrotron function plus blackbody, and the Band function (*18*). A blackbody component is not required when the more flexible Band function alone is used. Although the time evolution of E_{peak} as determined by Band function fits is consistent with a single power law (with an index of -0.96 ± 0.02), the evolution of the synchrotron peak energy is not (Fig. 2). A broken power-law fit is better constrained and shows a shallower decay before the pulse peak, with an index of -0.4 ± 0.2 during the rising phase and -1.17 ± 0.05 during the decaying phase and a fitted break time at $T_0 + 0.28 \pm 0.08$ s, or ~0.2 s before the pulse peak in the 10- to 1000-keV flux. Both fitted indices during the decay phase are consistent with the –1 power-law index expected from standard fireball curvature effects (*25*, *26*). The shallower spectral peak decay index before the light curve decay phase has a natural explanation in the context of the pulse being driven by a shock between thick, colliding shells (*19*).

Two-component models including a thermal contribution (*27*) constrain the value of the photospheric radius using the blackbody flux and temperature (kT) (see table S1). Comparing with the flux of the dominant nonthermal spectral component then permits determination of the Lorentz factor at the photosphere (Γ_{ph}) (*28*). As shown in Fig. 3, the minimum value of the photospheric bulk Lorentz factor Γ_{ph} starts out at 500 and monotonically decreases to ~100 over the duration of the pulse (similar to behavior observed in GRB 110721A) (*29*). Internal shocks require higher Lorentz factors at later times. However, this might still be consistent with the monotonically decreasing Γ_{ph} if the outflowing shell that produces this photospheric component produced the nonthermal triggering pulse by colliding with a slower and slightly earlier ejected shell that did not produce detectable photospheric emission. Otherwise, the observed behavior would favor magnetic reconnection models or mini-jets (*30*, *31*), which abandon a simple spherical geometry.

Using the measured redshift of $z = 0.34$ (*32*), the host rest-frame luminosity and synchrotron peak energies are calculated, and the decay-phase apparent isotropic luminosity L- E_{peak} correlation is fit with a power-law index of 1.43 ± 0.04 (Fig. 4). A theoretical analysis of high-latitude curvature radiation produced in relativistic shell collisions of spherical blast waves shows a $L \propto E_{peak}^{3}$ during the decay phase of a pulse (*25*, *26*), contrary to the behavior shown in Fig. 4. In a picture of an expanding fluid element rather than a colliding shell, synchrotron emission by electrons with characteristic energy γ_e obeys the relations $E_{peak} \propto \Gamma B \gamma_e^{2}$ and $L \propto \Gamma^2 B^2 \gamma_e^{2}$, for γ_e and B both in the jet frame. In the optically thin coasting phase of the outflow, the bulk Lorentz factor Γ

[1]Department of Space Science, University of Alabama in Huntsville, Huntsville, AL 35899, USA. [2]Center for Space Plasma and Aeronomic Research (CSPAR), University of Alabama in Huntsville, Huntsville, AL 35899, USA. [3]Max-Planck Institut für Extraterrestrische Physik, 85748 Garching, Germany. [4]University College Dublin, Belfield, Dublin 4, Ireland. [5]Universities Space Research Association (USRA), Columbia, MD 21044, USA. [6]NASA Marshall Space Flight Center, Huntsville, AL 35812, USA. [7]NASA Postdoctoral Program Fellow, USA. [8]Jacobs Technology, Huntsville, AL 35806, USA. [9]Los Alamos National Laboratory, Los Alamos, NM 87545, USA. [10]Astronomical Institute Anton Pannekoek University of Amsterdam, Postbus 94249 1090 GE Amsterdam, Netherlands. [11]Deutsches Elektronen Synchrotron DESY, D-15738 Zeuthen, Germany. [12]Space Sciences Laboratory, 7 Gauss Way, University of California, Berkeley, CA 94720–7450, USA. [13]Department of Astronomy, Stockholm University, SE-106 91 Stockholm, Sweden. [14]The Oskar Klein Centre for Cosmoparticle Physics, AlbaNova, SE-106 91 Stockholm, Sweden. [15]Department of Physics, Royal Institute of Technology (KTH), AlbaNova, SE-106 91 Stockholm, Sweden. [16]Università di Pisa and Istituto Nazionale di Fisica Nucleare, Sezione di Pisa I-56127 Pisa, Italy. [17]Istituto Nazionale di Fisica Nucleare, Sezione di Trieste, I-34127 Trieste, Italy. [18]Dipartimento di Fisica, Università di Trieste, I-34127 Trieste, Italy. [19]Rice University, Department of Physics and Astronomy, MS-108, P. O. Box 1892, Houston, TX 77251, USA. [20]Istituto Nazionale di Fisica Nucleare, Sezione di Padova, I-35131 Padova, Italy. [21]Dipartimento di Fisica e Astronomia G. Galilei, Università di Padova, I-35131 Padova, Italy. [22]Istituto Nazionale di Fisica Nucleare, Sezione di Pisa, I-56127 Pisa, Italy. [23]Institut für Astro- und Teilchenphysik and Institut für Theoretische Physik, Leopold-Franzens-Universität Innsbruck, A-6020 Innsbruck, Austria. [24]Istituto Nazionale di Fisica Nucleare, Sezione di Perugia, I-06123 Perugia, Italy. [25]Dipartimento di Fisica, Università degli Studi di Perugia, I-06123 Perugia, Italy. [26]Dipartimento di Fisica M. Merlin dell'Università e del Politecnico di Bari, I-70126 Bari, Italy [27]Istituto Nazionale di Fisica Nucleare, Sezione di Bari, 70126 Bari, Italy. [28]Laboratoire Leprince-Ringuet, École Polytechnique, CNRS/IN2P3, Palaiseau, France. [29]Institut de CiËncies de l'Espai (IEEE-CSIC), Campus UAB, 08193 Barcelona, Spain. [30]W. W. Hansen Experimental Physics Laboratory, Kavli Institute for Particle Astrophysics and Cosmology, Department of Physics and SLAC National Accelerator Laboratory, Stanford University, Stanford, CA 94305, USA. [31]INAF-Istituto di Astrofisica Spaziale e Fisica Cosmica, I-20133 Milano, Italy. [32]Center for Earth Observing and Space Research, College of Science, George Mason University, Fairfax, VA 22030, resident at Naval Research Laboratory, Washington, DC 20375, USA. [33]Agenzia Spaziale Italiana (ASI) Science Data Center, I-00044 Frascati (Roma), Italy. [34]Istituto Nazionale di Astrofisica, Osservatorio Astronomico di Roma, I-00040 Monte Porzio Catone (Roma), Italy. [35]Laboratoire Univers et Particules de Montpellier, Universitè Montpellier 2, CNRS/IN2P3, Montpellier, France. [36]Department of Physics and Astronomy, Sonoma State University, Rohnert Park, CA 94928–3609, USA. [37]Department of Physics, Stockholm University, AlbaNova, SE-106 91 Stockholm, Sweden. [38]Royal Swedish Academy of Sciences Research Fellow, funded by a grant from the K. A. Wallenberg Foundation. [39]The Royal Swedish Academy of Sciences, Box 50005, SE-104 05 Stockholm, Sweden. [40]INAF Istituto di Radioastronomia, 40129 Bologna, Italy. [41]Dipartimento di Fisica, Università di Udine and Istituto Nazionale di Fisica Nucleare, Sezione di Trieste, Gruppo Collegato di Udine, I-33100 Udine, Italy. [42]Space Science Division, Naval Research Laboratory, Washington, DC 20375–5352, USA. [43]Department of Physical Sciences, Hiroshima University, Higashi-Hiroshima, Hiroshima 739-8526, Japan. [44]NASA Goddard Space Flight Center, Greenbelt, MD 20771, USA. [45]Department of Natural Sciences, The Open University of Israel, 1 University Road, POB 808, Ra'anana 43537, Israel. [46]Laboratoire AIM, CEA-IRFU/CNRS/Universitè Paris Diderot, Service d'Astrophysique, CEA Saclay, 91191 Gif sur Yvette, France. [47]Department of Astronomy, Graduate School of Science, Kyoto University, Sakyo-ku, Kyoto 606-8502, Japan. [48]Science Institute, University of Iceland, IS-107 Reykjavik, Iceland. [49]CNRS, Institut de Recherche en Astrophysique et Planétologie (IRAP), F-31028 Toulouse cedex 4, France. [50]Galaxies, Astrophysique des Hautes Energies et Cosmologie (GAHEC), Universitè de Toulouse, UPS-OMP, IRAP, Toulouse, France. [51]Istituto Nazionale di Fisica Nucleare, Sezione di Torino, I-10125 Torino, Italy. [52]Hiroshima Astrophysical Science Center, Hiroshima University, Higashi-Hiroshima, Hiroshima 739-8526, Japan. [53]Istituto Nazionale di Fisica Nucleare, Sezione di Roma Tor Vergata, I-00133 Roma, Italy. [54]Institute of Space and Astronautical Science, Japan Aerospace Exploration Agency (JAXA), 3-1-1 Yoshinodai, Chuo-ku, Sagamihara, Kanagawa 252-5210, Japan. [55]Solar-Terrestrial Environment Laboratory, Nagoya University, Nagoya 464-8601, Japan. [56]Max-Planck-Institut für Physik, D-80805 München, Germany. [57]Department of Physics and Center for Space Sciences and Technology, University of Maryland Baltimore County, Baltimore, MD 21250, USA. [58]Center for Research and Exploration in Space Science and Technology (CRESST) and NASA Goddard Space Flight Center, Greenbelt, MD 20771, USA. [59]Santa Cruz Institute for Particle Physics, Department of Physics and Department of Astronomy and Astrophysics, University of California at Santa Cruz, Santa Cruz, CA 95064, USA. [60]University of Johannesburg, Department of Physics, University of Johannesburg, Auckland Park 2006, South Africa. [61]Department of Physics, University of Washington, Seattle, WA 98195–1560, USA. [62]Space Sciences Division, NASA Ames Research Center, Moffett Field, CA 94035–1000, USA. [63]NYCB Real-Time Computing Inc., Lattingtown, NY 11560–1025, USA. [64]Department of Chemistry and Physics, Purdue University Calumet, Hammond, IN 46323–2094, USA. [65]Institució Catalana de Recerca i Estudis Avançats (ICREA), Barcelona, Spain. [66]Department of Physics and Department of Astronomy, University of Maryland, College Park, MD 20742, USA. [67]Consorzio Interuniversitario per la Fisica Spaziale (CIFS), I-10133 Torino, Italy. [68]Dipartimento di Fisica, Università di Roma "Tor Vergata", I-00133 Roma, Italy. [69]Department of Physics, Center for Cosmology and Astro-Particle Physics, The Ohio State University, Columbus, OH 43210, USA.

*Corresponding author. E-mail: preecer@uah.edu (R.P.); James.Burgess@uah.edu (J.M.B.); charles.dermer@nrl.navy.mil (C.D.D); nicola.omodei@stanford.edu (N.O.); azk@mpe.mpg.de (A.v.K.)

is constant. Naively assuming that the magnetic flux is frozen in the flow ($BR^2 \propto$ const. in the comoving frame, where R is the comoving emission region radius), then adiabatic losses of the electrons imply $\gamma_e \propto R^{-1}$. A short calculation then gives $L \propto E_{peak}^{3/2}$, which is consistent with the 1.43 index derived from the data. A constant expansion velocity dR/dt scenario predicts, however, $E_{peak} \propto R^{-4} \propto t^{-4}$. Other jet-wind assumptions

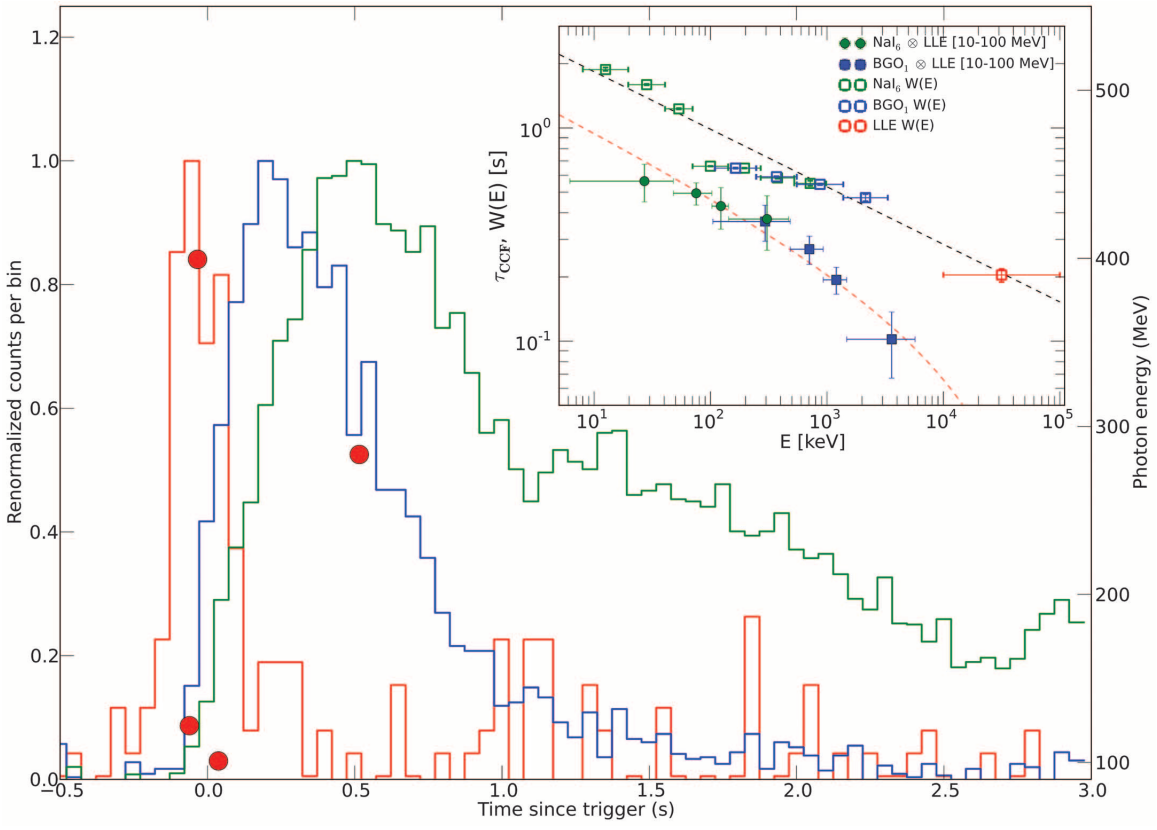

Fig. 1. The first 3 s of GRB 130427A. Shown, are composite light curves for the three Fermi detector types. Green, GBM NaI #6 (10 to 300 keV); blue, GBM BGO #1 (300 keV to 45 MeV); red, LAT LLE (>20 MeV). Each curve has been normalized so that their peak intensities match. High-probability LAT photons >100 MeV are indicated by circles (right axis, energy in MeV). (Inset) Lag analysis of the triggering pulse of GRB 130427A. Time lag τ (filled symbols) as determined by the DCCF analysis between the (10 to 100 MeV) LLE light curve and selected energy bands of the NaI (green) and BGO (blue) light curves. Also displayed are fitted pulse widths as a function of energy $W(E)$ (hollow symbols, in seconds) for several energy bands. The two dashed lines represent: 1, the best-fit power-law model (χ^2 of 5.6 for 9 degrees of freedom) for $W(E)$ (black), and 2, the expected dependence of the time lag τ as a function of energy (red), assuming the same power-law index as in 1.

Fig. 2. The fitted Band function E_{peak} (blue) and synchrotron peak energies (red) as a function of time. The times are referenced from when the LLE light curve peaks 0.1 s before the trigger. A broken power-law fit to the red points is indicated by a dashed line (early time decay index of -0.4 ± 0.2, with a break at 0.38 ± 0.08 s, breaking to an index of -1.17 ± 0.05 with a $\chi^2 = 28$ for 22 degrees of freedom). We also show the Band function E_{peak} values for the same time intervals with a single fitted power-law index (-0.96 ± 0.02 with a χ^2 of 19 for 24 degrees of freedom).

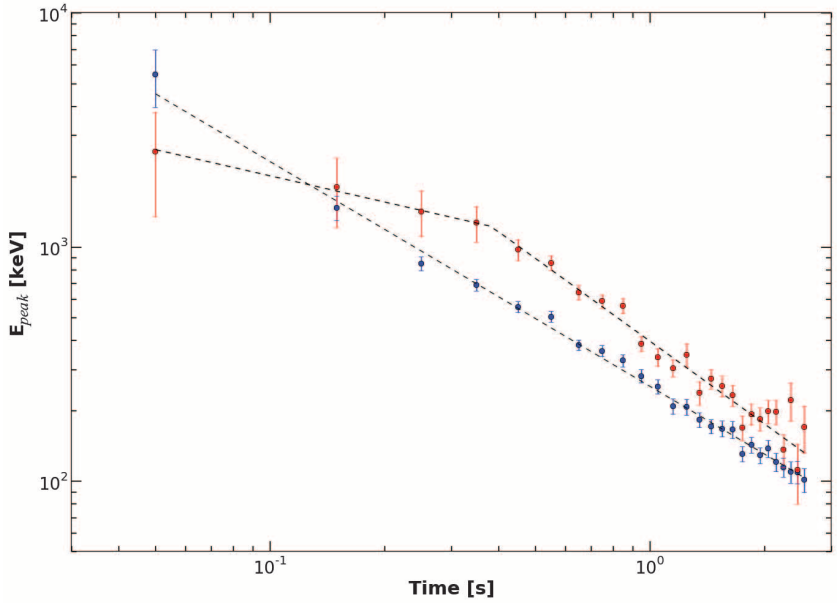

yield different correlations—for example, for the deceleration epoch where $d\Gamma/dt < 0$ or for radial field evolution appropriate for jet cores.

The isolated initial pulse of GRB 130427A is apparently unmodified by preceding engine activity or nascent external shock emission. Our analysis shows that there is good agreement between the pulse width as a function of energy and the expected lag, that the characteristic energy has roughly a –1 power-law decay with time during the decaying phase, that the temperature of the blackbody component implies a photospheric radius incompatible with the internal shock radius, and that the apparent isotropic luminosity is related to the 3/2 power of the characteristic energy. It is a challenge to explain all these behaviors simultaneously.

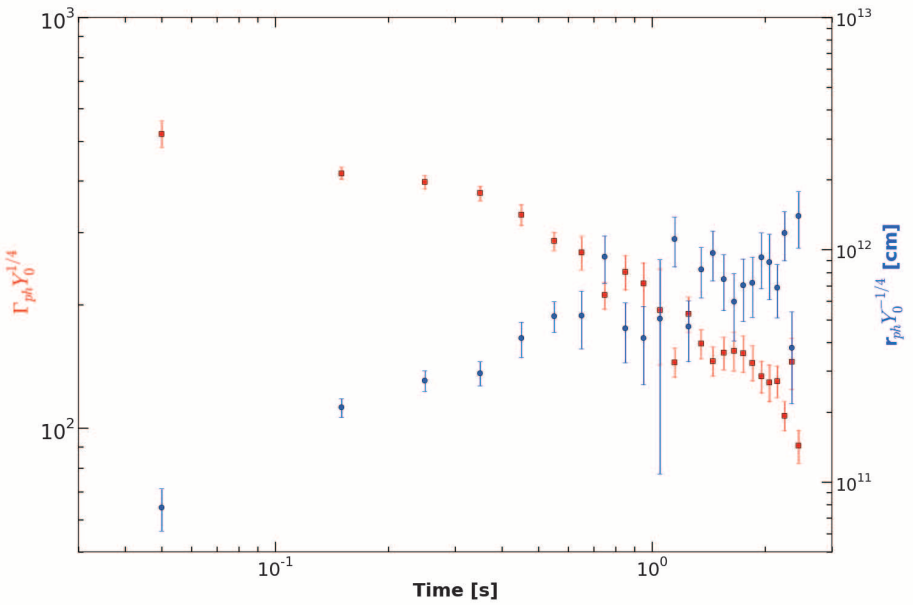

Fig. 3. Plot showing trends in the derived photospheric Lorentz factor (red, left axis) and radius (blue, right axis). The reference time is the same as in Fig. 2. We obtain both values from the instantaneous ratio of the observed blackbody component flux to the total flux, following equations 4 and 5 in (*28*) and assuming a value of 1 for the ratio between the total emitted thermal energy versus the total energy emitted in gamma rays (Y_0).

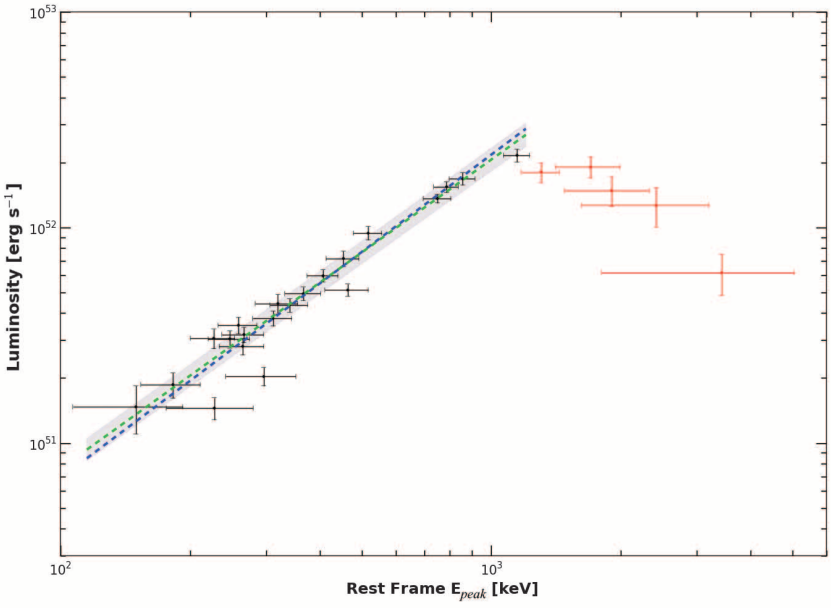

Fig. 4. Correlation between the GRB 130427A host rest frame synchrotron peak energy and isotropic luminosity during the rising phase (red) and decaying phase (black) of the triggering pulse. Time progresses approximately from right to left on the plot. The 1.43 ± 0.04 power-law index fit to the black points is shown in green (region of uncertainty in gray), and the 3/2 power law from the magnetic flux-freezing calculation in the text is indicated in blue.

References and Notes

1. C. Meegan *et al.*, *Astrophys. J.* **702**, 791–804 (2009).
2. A. Maselli *et al.*, *GCN Cir.* **2013**, 14448 (2013); http://gcn.gsfc.nasa.gov/gcn3/14448.gcn3.
3. S. Zhu *et al.*, *GCN Cir.* **2013**, 14471 (2013); http://gcn.gsfc.nasa.gov/gcn3/14471.gcn3.
4. A. von Kienlin, *GCN Cir.* **2013**, 14473 (2013); http://gcn.gsfc.nasa.gov/gcn3/14473.gcn3.
5. S. Golenetskii *et al.*, *GCN Cir.* **2013**, 14487 (2013); http://gcn.gsfc.nasa.gov/gcn3/14487.gcn3.
6. M. Axelsson *et al.*, *Astrophys. J.* **757**, L31 (2012).
7. W. S. Paciesas *et al.*, *Astrophys. J.* **199** (suppl.), 18 (2012).
8. Fermi GBM Online Burst Catalog, http://heasarc.gsfc.nasa.gov/W3Browse/fermi/fermigbrst.html.
9. Compton Science Support Center BATSE Online Burst Catalog, http://heasarc.gsfc.nasa.gov/docs/cgro/batse.
10. M. Ackermann *et al.*, *Science* **343**, 42–47 (2014).
11. A. Maselli *et al.*, *Science* **343**, 48–51 (2014).
12. L. A. Ford *et al.*, *Astrophys. J.* **439**, 307 (1995).
13. R.-J. Lu, S.-J. Hou, E.-W. Liang, *Astrophys. J.* **720**, 1146–1154 (2010).
14. V. Pelassa, R. Preece, F. Piron, N. Omodei, S. Guiriec, arXiv:1002.2617 (2010).
15. M. Ackermann *et al.*, *Astrophys. J.* **745**, 144 (2012).
16. R. A. Edelson, J. H. Krolik, *Astrophys. J.* **333**, 646 (1988).
17. J. P. Norris *et al.*, *Astrophys. J.* **459**, 393 (1996).
18. For details, see the Spectral Analysis Method section in the supplementary materials on *Science* Online.
19. F. Daigne, R. Mochkovitch, *Mon. Not. R. Astron. Soc.* **296**, 275–286 (1998).
20. D. Band *et al.*, *Astrophys. J.* **413**, 281 (1993).
21. S. Guiriec *et al.*, *Astrophys. J.* **727**, L33 (2011).
22. S. Guiriec *et al.*, *Astrophys. J.* **770**, 32 (2013).
23. J. M. Burgess *et al.*, *Astrophys. J.* **741**, 24 (2011).
24. J. M. Burgess *et al.*, arXiv:1304.4628 (2013).
25. C. D. Dermer, *Astrophys. J.* **614**, 284–292 (2004).
26. F. Genet, J. Granot, *Mon. Not. R. Astron. Soc.* **399**, 1328–1346 (2009).
27. F. Ryde, *Astrophys. J.* **614**, 827–846 (2004).
28. A. Pe'er, F. Ryde, R. A. M. J. Wijers, P. Mészáros, M. J. Rees, *Astrophys. J.* **664**, L1–L4 (2007).
29. S. Iyyani *et al.*, *Mon. Not. R. Astron. Soc.* **433**, 2739–2748 (2013).
30. B. Zhang, H. Yan, *Astrophys. J.* **726**, 90 (2011).
31. M. Lyutikov, R. Blandford, arXiv:astro-ph/0312347 (2003).
32. A. J. Levan *et al.*, *GCN Cir.* **2013**, 14455 (2013).

Acknowledgments: The Fermi data are publically available at NASA's Fermi Science Support Center's Web site: http://fermi.gsfc.nasa.gov/ssc. The Fermi GBM collaboration acknowledges support for GBM development, operations, and data analysis from NASA in the United States and BMWi/DLR in Germany. The Fermi LAT Collaboration acknowledges support from a number of agencies and institutes for both development and the operation of the LAT, as well as scientific data analysis. These include NASA and the Department of Energy in the United States; CEA/Irfu and IN2P3/CNRS in France; ASI and INFN in Italy; MEXT, KEK, and JAXA in Japan; and the K. A. Wallenberg Foundation, the Swedish Research Council, and the National Space Board in Sweden. Additional support from INAF in Italy and CNES in France for science analysis during the operations phase is also gratefully acknowledged.

Supplementary Materials

www.sciencemag.org/content/343/6166/51/suppl/DC1
Supplementary Text
Table S1
References (*33*–*35*)

24 June 2013; accepted 23 October 2013
Published online 21 November 2013;
10.1126/science.1242302